

Research Article

Millimeter-Wave Ultra-Wideband Six-Port Receiver Using Cross-Polarized Antennas

Nazih Khaddaj Mallat,¹ Emilia Moldovan,¹ Ke Wu,² and Serioja O. Tatu¹

¹ Université du Québec, Institut National de la Recherche Scientifique, Centre Énergie, Matériaux et Télécommunications (INRS-EMT), 800 de la Gauchetière Ouest, R 6900 Montréal, QC, Canada H5A 1K6

² Centre de Recherche Poly-Grames, Ecole Polytechnique de Montréal, Montréal, QC, Canada H3T 1J4

Correspondence should be addressed to Nazih Khaddaj Mallat, nazih@ieee.org

Received 19 January 2009; Revised 4 May 2009; Accepted 3 July 2009

Recommended by Claude Oestges

This paper presents a new low-cost millimeter-wave ultra-wideband (UWB) transceiver architecture operating over V-band from 60 to 64 GHz. Since the local oscillator (LO) power required in the operation of six-port receiver is generally low (compared to conventional one using diode mixers), the carrier recovery or LO synchronization is avoided by using second transmission path and cross-polarized antennas. The six-port model used in system simulation is based on *S*-parameters measurements of a rectangular waveguide hybrid coupler. The receiver architecture is validated by comparisons between transmitter and receiver bit sequences and bit error rate results of 500 Mb/s pseudorandom QPSK signal.

Copyright © 2009 Nazih Khaddaj Mallat et al. This is an open access article distributed under the Creative Commons Attribution License, which permits unrestricted use, distribution, and reproduction in any medium, provided the original work is properly cited.

1. Introduction

Due to a rapid growth of high-speed wireless technologies, new wireless systems at home and corporate environment are expected to emerge in the near future. This increasing interest for ultra-high-speed wireless connectivity has pushed the Federal Communications Commission (FCC) to provide new opportunities for unlicensed spectrum usage with fewer restrictions on radio parameters. The Ultra-Wideband (UWB) technology, proposed for high-speed short-range applications, used both the occupied and unoccupied spectrum across the 3.1–10.6 GHz band. Conventional microwave UWB technology (3.1–10.6 GHz band) is one of the most active focus areas in academia, industry, and regulatory circles. Because of the power spectral density limitations (−41 dBm/MHz), the microwave UWB overlays existing wireless services (GPS, PCS, Bluetooth, and IEEE 802.11 WLANs) without significant interferences. Compared to this low-frequency range UWB technology, 60 GHz millimeter-wave communications will operate in the currently unlicensed spectrum (57–64 GHz), where the oxygen absorption limits a long-distance interference [1–6].

The multipoint quadrature down-conversion has been demonstrated to provide an innovative approach to the design of high-speed and low-cost wireless systems. It is known that millimeter-wave technology enables the design of compact and low-cost wireless transceivers which can permit convenient terminal mobility up to Gb/s data-rates. Various millimeter-wave front-end architectures, fabrication technologies, simulations, and measurements based on multipoint have been proposed and developed in recent years [7–11]. In [12], it was demonstrated that the six-port mixer is less sensitive to the LO signal power variations than its conventional counterpart using antiparallel diodes.

In order to avoid tedious carrier recovery or expensive millimeter-wave local oscillator synchronization techniques, and due to the specific six-port properties [12], we propose, in this work, a new low-cost homodyne receiver architecture. Since the six-port receiver does not require a high LO power to fulfill the millimeter-wave receiver task, both reference (LO) and modulated radio-frequency (RF) signals can be transmitted through cross-polarized antennas [13]. In order to validate this proposed approach, a set of system simulations are performed. For creating more realistic results,

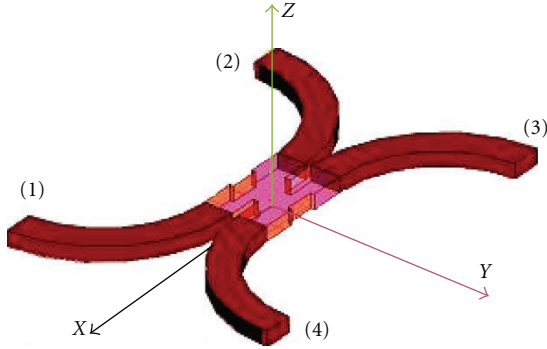


FIGURE 1: Layout of the RWG 90° hybrid coupler.

the six-port model used in these simulations is based on the actual S -parameters measurements of a wideband 90° hybrid coupler, using the rectangular waveguide technology (RWG). In the first part, the measurement results of a V-band 90° hybrid coupler and the simulation results of the proposed six-port model based on previous measurements are presented. Furthermore, a communication link has been simulated using a 500 Mb/s quadrature phase shift keying (QPSK) modulated signal.

2. Six-Port Proposed Model

2.1. Hybrid Coupler Measurements. A new V-band 90° hybrid coupler is designed and fabricated, in a metal block of brass, using WR-12 standard rectangular waveguide technology, suitable for V-band (50–75 GHz) millimeter-wave design and applications. The commercial software High-Frequency Structure Simulator (HFSS) of Ansoft Corporation is used for the coupler design. Figure 1 shows the layout of this coupler.

All of the four ports allow access by the standard WR-12 flanges connected to the measurement equipment. The S -parameters of the WR-12 coupler are measured using the Agilent Technologies 60–90 GHz millimeter-wave power network analyser (PNA, model E8362B).

Figure 2 shows measured transmissions S_{12} and S_{13} , isolation S_{23} and return loss S_{11} . Similar results have been obtained for other ports due to the circuit symmetry. The measured isolation between ports 2–3 is better than 30 dB. The measured power split and return loss (S_{11}) versus frequency are $[-4$ to $-7]$ dB and -24 dB, respectively. All these measured results are obtained for a large bandwidth frequency of 10 GHz (60–70 GHz). This considerable huge bandwidth gives us many advantages to enable the six-port model based on these coupler measurements results. As the regulatory bandwidth defined, in North America, around 60 GHz is [57–64 GHz] and due to our network analyzer measurements limitations (millimeter-wave modules from 60 to 90 GHz), all our following results and measurements will be considered for the bandwidth range [60–64 GHz].

In addition, Figure 3 shows that the phases of transmission scattering S -parameters (S_{12} and S_{13}) present a very good linearity and a constant difference of around 90° over the considered band.

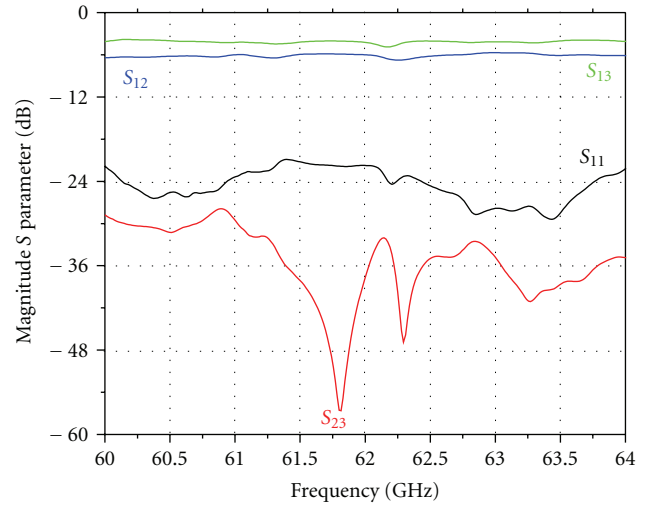


FIGURE 2: Magnitude S -parameters measurements results of the transmission, return loss, and isolation.

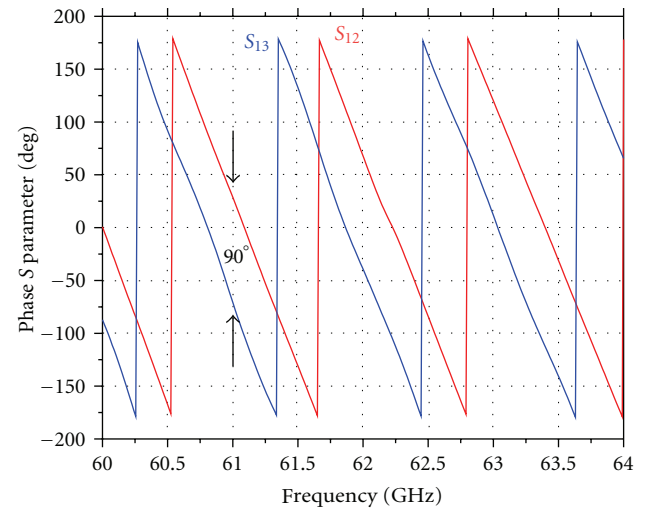


FIGURE 3: Measurements results of the transmission S -parameters phases: RWG coupler.

2.2. Six-Port Simulation. Through earlier publications [7, 8], two different six-port prototypes were proposed. A ka-band (27 GHz) six-port model composed of a Wilkinson power divider and three 90° was fabricated and measured in [7]. Furthermore, a V-band (60 GHz) six-port device composed of four 90° hybrid couplers but based only on simulations results is proposed in [8]. In this paper, we enhance the previous work by providing a more realistic simulation of the six-port circuit, since it is based on the measured S -parameters of the fabricated RWG 90° directional couplers. Then, it is implemented using Advanced Design Systems (ADS) software of Agilent Technologies. The block diagram of the six-port circuit, used in this paper, is the same presented in [8]. It is composed of four 90° hybrid couplers and a 90° phase shifter, as shown in Figure 4. The RF Input and RF reference LO signals, related to the two input

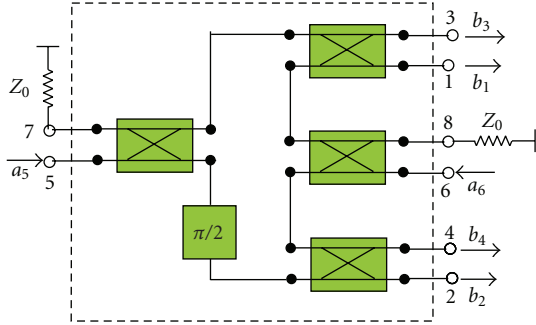


FIGURE 4: Six-port circuit block diagram.

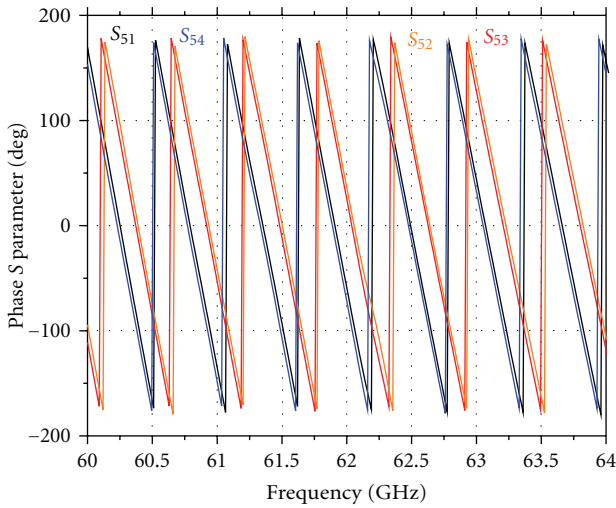


FIGURE 5: S-parameters transmission phases: six-port.

normalized waves a_5 and a_6 , are connected to ports 5 and 6. The outputs ports are nominated 1, 2, 3, and 4.

S-parameters simulations of this six-port are accomplished in ADS. The phase S-parameters are described in Figure 5. The phases of S_{51} and S_{52} are equal as well as phases of S_{53} and S_{54} . Ports (1,2) and ports (3,4) are 90° out of phase over a very wide band, suitable for a high-quality I/Q mixer. Respectively, we obtain 20 dB of matching, more than 30 dB of isolation between input ports and $[-8$ to $-12]$ dB of coupling between output ports as shown in Figures 6 and 7.

Following the mathematical equations discussed in [7, 8], the coupling factor of the six-port should be around -6 dB (one-quarter power or 25%). This difference in value is related to the fact that, due to the fabrication errors in the RWG coupler, the coupling factor obtained is $[-4$ to $-7]$ dB (see Figure 2). Theoretically, this should be -3 dB for the coupler itself. This coupling factor mismatch will not affect the demodulator process since the phases between the outputs ports are shifted by multiple of 90° as shown in Figure 5, and this is the important criteria for our receiver demodulator.

According to [7, 8], in order to obtain the dc output signals, four power detectors are connected to the six-port outputs. The I/Q down-converted signals are obtained using

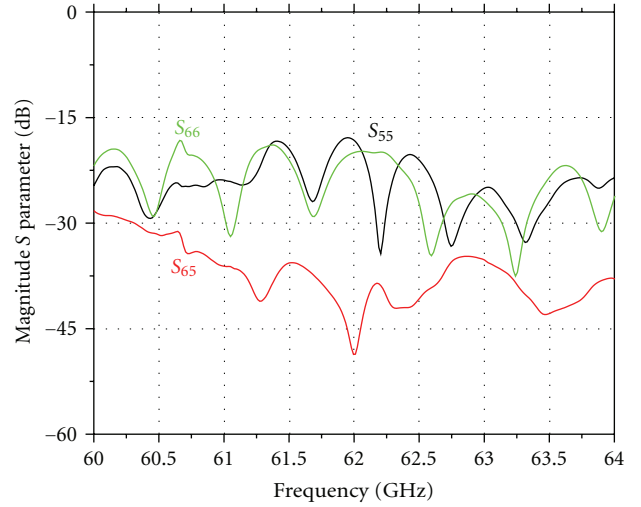


FIGURE 6: Magnitude S-parameters return loss and isolation: six-port.

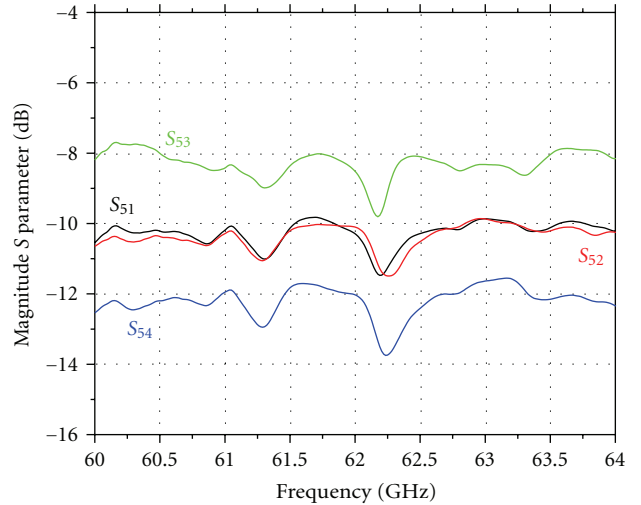


FIGURE 7: Magnitude S-parameters transmission: six-port.

a differential approach, as shown in (1), where K is a constant, I/Q (In-phase/Quadrature-phase) signals, V_1 to V_4 are the multipoint output detected signals, a is the amplitude of the LO signal, $\Delta\varphi(t) = \varphi_6(t) - \varphi_5$ is the instantaneous phase difference, and $\alpha(t)$ is the instantaneous amplitude ratio between the RF and LO signals:

$$\begin{aligned} I(t) &= V_3(t) - V_1(t) = K \cdot \alpha(t) \cdot |a|^2 \cdot \cos[\Delta\varphi(t)], \\ Q(t) &= V_4(t) - V_2(t) = K \cdot \alpha(t) \cdot |a|^2 \cdot \sin[\Delta\varphi(t)]. \end{aligned} \quad (1)$$

In order to validate the six-port model, a harmonic balance simulation is performed. The phase between RF and LO signals is swept in a 360° range, and the RF and LO levels are set at -10 dBm. The RF six-port output voltage magnitude variations (V_1 to V_4) versus this phase shift are shown in Figure 8. Theoretically, due to the use of 90° hybrid couplers, periodical maximal and minimal (zero) values

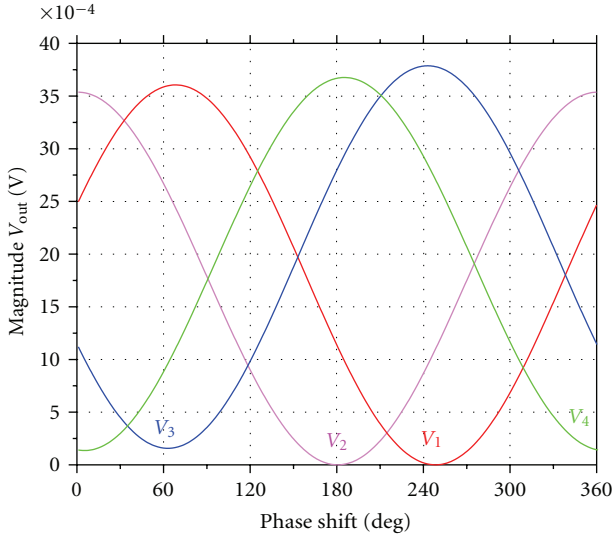


FIGURE 8: Harmonic balance simulation results of V_{out} magnitude versus RF input phase.

should be obtained for each output voltage. The minimal magnitude values are shifted by 90° multiples, as required for I/Q mixers. Practically, due to circuit's inherent amplitude and phase unbalances over the frequency band, nonzero minimum values are generated and some phase difference errors between minimums appear, as seen in Figure 8.

As detailed in [7, 8], for a I/Q six-port down-converter, the output magnitude voltage differences ($V_1 - V_3$) and ($V_4 - V_2$) are related to I , Q outputs signals, respectively. Figure 8 shows a phase difference of approximately 180° between V_1 and V_3 , and also between V_4 and V_2 , as required. In addition, around 90° phase difference is obtained between quadrature outputs.

Figure 9 shows the percentage of the quadrature outputs phase difference error (related to 180°), in the 4 GHz band. This phase error, between 2% and 7%, is considered favorable result for the use of the proposed six-port circuit in QPSK signal demodulations over the entire 4 GHz band, from 60 to 64 GHz.

3. New Six-Port Receiver Architecture

Since the free space loss increases quadratically with operating frequency, the V-band frequencies are dedicated to very short-range wireless communications (up to 10 m).

In a previous publication [7], demodulation results were presented for a millimeter wave homodyne receiver based on a six-port down-converter, considering a perfect synchronism. Signal processing techniques were used to synchronize the reference signal using a feedback from the signal processing circuit to the millimeter-wave LO. Moreover, a carrier recovery process in a V-band millimeter wave six-port heterodyne receiver has been presented in [10], and a typical analog carrier recovery circuit was proposed in [14] for a QPSK modulation through an homodyne architecture.

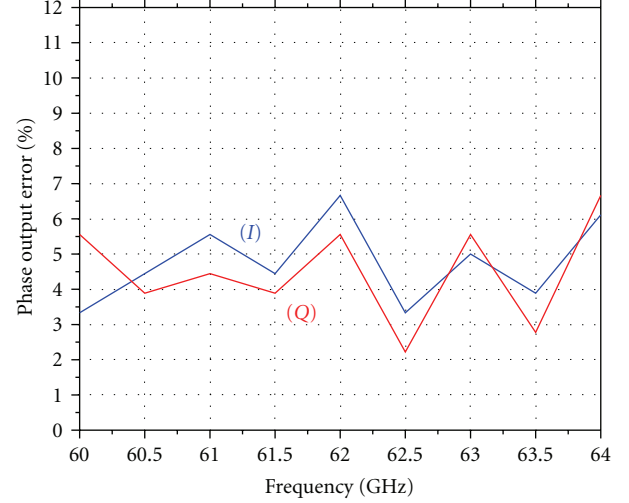


FIGURE 9: Quadrature signals phase output error (%).

However, these techniques are relatively expensive and also reduce the maximum bit-rate, due to the analog to digital conversion and signal processing algorithms.

Based on previous comments, in order to obtain a low-cost solution of the LO synchronism problem, we propose the use of a second millimeter-wave link for the unmodulated signal and cross-polarized antennas, as shown in Figure 10. In the transmitter part, the LO and RF signals are radiated through two similar cross polarized antennas. At the receiver part, an identical couple of antennas are used.

As is known, if both antennas have the same polarization, the angle between their radiated E-fields is zero, and there is no power loss due to polarization mismatch. The polarization loss factor (PLF) or polarization mismatch loss (PML) will characterize the power loss due to the polarization mismatch. The PLF loss factor dictates what portion of the incident power is captured by the receiver antenna. This is often less than unity and depends on the angle between the transmitted signal polarization and the receiver antenna polarization. In our case, two pairs of transmitting/receiving antennas are vertically and, respectively, horizontally polarized. Hence, the angle between the antennas is 90° , and no power will be transferred between more than two antennas in the same time. In fact, the six-port circuit is an RF six-port interferometer with a variety of architectures consisting of power dividers, couplers, and phase shifters. These RF components are interconnected in such a way that four different vector sums of reference signal and signal to be directly measured (or down-converted) are produced. Magnitude and phase of unknown signal are determined from amplitudes of four output signals from interferometer. So, the relative rotation between the transmitting and the receiving antennas will not affect our goal. The RF and LO signals are received on ports 5 and 6 of the six-port, respectively. If the antennas are rotated, we still may receive the two signals but on reverse ports (RF on port 6 and LO on port 5), since the transmitting and receiving antennas are cross-polarized.

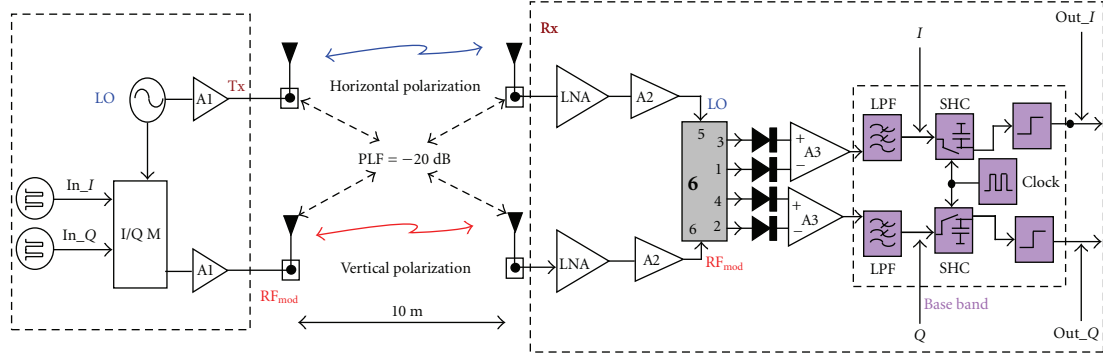


FIGURE 10: V-band six-port receiver proposed architecture.

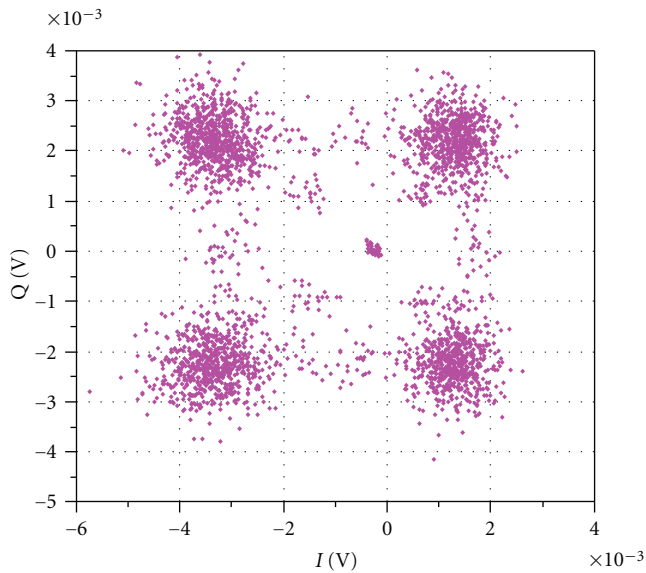


FIGURE 11: Demodulated 500 Mb/s QPSK signals (six-port output).

4. Demodulation Results

System simulations are performed using ADS, in order to validate the proposed architecture. During these simulations, we tried to get close as much as we can to the realistic properties of each component. For this reason, we have considered a PLF factor for the antennas, six-port based on coupler measurements results, amplifiers with acceptable gains, and the diodes spice models for the power detectors. The LO and RF transmitted signal powers are set at 10 dBm, and the antenna gains are 10 dBi. Since the antennas are cross-polarized, a PLF value of -20 dB is used in the simulations. This PLF value is commonly considered for cross-polarized antennas with a similar gain (10 dBi). A loss-link model based on the Friis equation is used to simulate the signal propagation over a distance d of 10 m. The free loss at 61 GHz is 88 dB; it is calculated using the Friis transmission equation in (2):

$$\frac{P_r}{P_t} = G_t G_r \left(\frac{\lambda}{4\pi R} \right)^2, \quad (2)$$

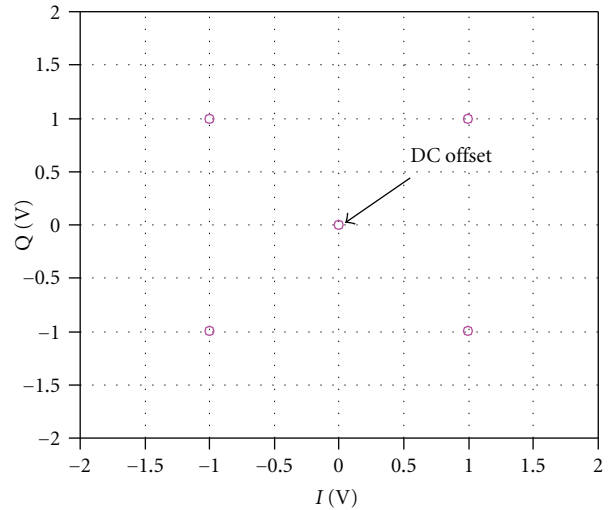


FIGURE 12: Demodulated 500 Mb/s QPSK signals (baseband output).

where P_r is the power received by the receiving antenna, and P_t is the power input to the transmitting antenna. G_t and G_r are the antenna gain of the transmitting and receiving antennas, respectively, λ is the wavelength (around 5 mm for 60 GHz), and R is the distance (10 m).

The ADS-based receiver model is composed of the six-port model constructed on the measurement results of the RWG 90° hybrid coupler, two pairs of cross-polarized antennas, four power detectors, low-noise amplifiers (LNAs), millimeter-wave amplifiers A2, and baseband amplifiers A3 (gains of 5 dB, 25 dB, and 30 dB, resp.) and low pass filters (LPF). The sample-and-hold circuits (SHCs) and the limiters are used to obtain a clearly demodulated constellation (without the transitions between consecutive states). The two antennas are in unobstructed free space, with no multipath and considered as lossless and oriented for maximum response.

An ADS envelope simulation at the carrier frequency of 61 GHz is performed using the block diagram of Figure 10. As the receiver reference signal is obtained from the transmitter LO signal, there are no synchronism problems. Based

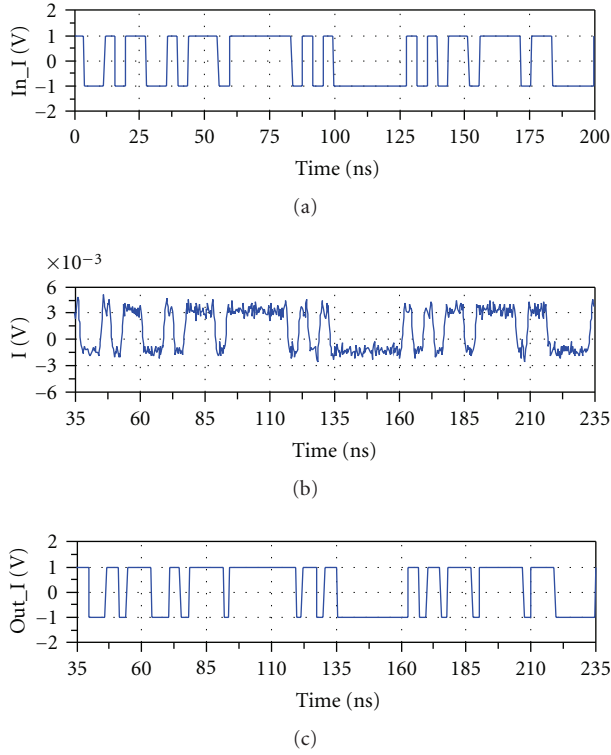


FIGURE 13: Demodulation results of 250 Mb/s QPSK pseudorandom (I) bit sequence: (a) transmitted, (b) received, after LPF, (c) demodulated, at limiter output.

on the power evaluation, the LO and RF signals at the six-port inputs are around -28 dBm:

- (i) $+10$ dBm (transmitted signal power defined by FCC for V-band communications systems [4]),
- (ii) $+10$ dBi (antenna gain),
- (iii) -88 dB (path loss calculated using (2)),
- (iv) $+10$ dBi (antenna gain),
- (v) $+5$ dB (LNA gain),
- (vi) $+25$ dB (A2 gain).

A pseudorandom 500 Mbps QPSK signal is used to validate the principle of operation. Figures 11 and 12 show the demodulated constellations using the proposed architecture for high-speed (500 Mb/s) QPSK signal, at the output of the six-port and the output of the baseband part, respectively. Due to the differential approach used and (1), the DC offset value obtained theoretically is null. However, because of the S -parameters measurements results of the hybrid coupler used to simulate the six-port circuit and the simulations specifications (sampling higher than bit rate), the DC offset is not zero and it represents the transition between different states across the origin of the constellation. Through these two figures, we can see the role done by the SHCs/limiters to obtain a clear and net QPSK constellation.

Figures 13 and 14 show the input and demodulated signals of I and Q channels, respectively, for a bit sequence of

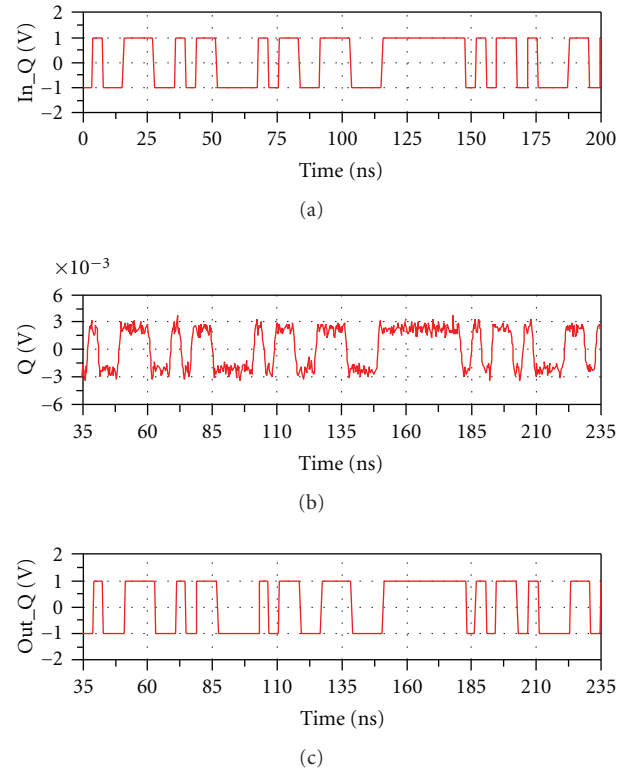


FIGURE 14: Demodulation results of 250 Mb/s QPSK pseudorandom (Q) bit sequence: (a) transmitted, (b) received, after LPF, (c) demodulated, at limiter output.

200 nanoseconds. As can be seen, the demodulated signals, at the limiter output, have exactly the same bit sequence as those transmitted, which has confirmed the successful demodulation. The delay of 33 nanoseconds is observed due to the propagation for a distance $d = 10$ m.

Figure 15 shows the bit error rate (BER, the number of bit errors divided by the total number of bits transmitted) variation versus the energy per bit to the spectral noise density (E_b/N_0) for the same distance of 10 m. It can be seen that the (E_b/N_0) required for BER of 10^{-9} is equal to 13 dB. It is an acceptable result based on the power energy balance calculated in [12]. The proposed receiver has a high BER performance (close to the theoretical one). This result demonstrates its capability for use in wireless HD (High Definition) video communications, which typically require much lower BER (10^{-8} to 10^{-9}) values than audio reception requires (around 10^{-4}), because video is much more sensitive to bit errors than audio is [15].

5. Conclusion

In this paper, a class of new low-cost six-port homodyne receiver architectures has been presented and demonstrated at millimeter-wave frequencies. Cross-polarized antennas are used at both transmitter and receiver in order to easily solve the severe LO synchronism problem in V-band. So as to obtain realistic system simulation results, the proposed

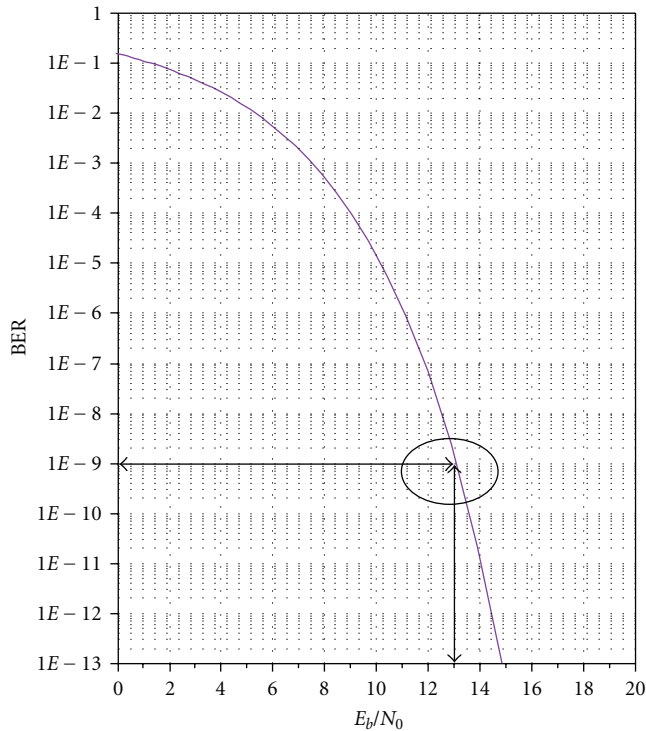


FIGURE 15: BER results for 500 Mb/s QPSK signal.

millimeter-wave UWB six-port receiver model is based on measurements of a fabricated V-band RWG 90° hybrid coupler. Even with the presence of some errors due to fabrication errors, the proposed receiver architecture validates excellent demodulation results in a band of 4 GHz [60–64 GHz]. ADS simulations are performed to analyse the proposed six-port architecture.

As demonstrated in this paper, this wireless proposed system is able to transmit 500 Mb/s data-rate with a BER of 10^{-9} up to 10 m range, as required for the wireless HDTV (High-Definition TV) specifications in indoor communications. It enables the design of high-performance, compact, and low-cost wireless millimeter-wave communication receivers for future high-speed wireless communication systems.

Acknowledgment

The authors gratefully acknowledge the financial support of the “Fonds Québécois de la Recherche sur la Nature et les Technologies, FQRNT/NATEQ.”

References

- [1] FCC, et al., “First report and order,” Tech. Rep. FCC 02-48, February 2002.
- [2] D. Porcino, W. Hirt, et al., “Ultra-wideband radio technology: potential and challenges ahead,” *IEEE Communications Magazine*, vol. 41, no. 7, pp. 66–74, 2003.
- [3] A. F. Molisch, J. R. Foerster, and M. Pendergrass, “Channel models for ultrawideband personal area networks,” *IEEE Wireless Communications*, vol. 10, no. 6, pp. 14–21, 2003.
- [4] P. Smulders, “Exploiting the 60 GHz band for local wireless multimedia access: prospects and future directions,” *IEEE Communications Magazine*, vol. 40, no. 1, pp. 140–147, 2002.
- [5] D. Cabric, M. S. W. Chen, D. A. Sobel, S. Wang, J. Yang, and R. W. Brodersen, “Novel radio architectures for UWB, 60 GHz, and cognitive wireless systems,” *EURASIP Journal on Wireless Communications and Networking*, vol. 2006, Article ID 17957, 18 pages, 2006.
- [6] C. Park and T. S. Rappaport, “Short-range wireless communications for next-generation networks: UWB 60 GHz millimeter-wave wpan, and ZigBee,” *IEEE Wireless Communications*, vol. 14, no. 4, pp. 70–78, 2007.
- [7] S. O. Tatu, E. Moldovan, K. Wu, R. G. Bosisio, and T. A. Denidni, “Ka-band analog front-end for software-defined direct conversion receiver,” *IEEE Transactions on Microwave Theory and Techniques*, vol. 53, no. 9, pp. 2768–2776, 2005.
- [8] S. O. Tatu and E. Moldovan, “V-band multi-port heterodyne receiver for high-speed communication systems,” *EURASIP Journal on Wireless Communications and Networking*, vol. 2007, Article ID 34358, 7 pages, 2007.
- [9] E. Moldovan, S. O. Tatu, and S. Affes, “A 60 GHz multi-port front-end architecture with integrated phased antenna array,” *Microwave and Optical Technology Letters*, vol. 50, no. 5, pp. 1371–1376, 2008.
- [10] N. K. Mallat and S. O. Tatu, “Carrier recovery loop for millimeter-wave heterodyne receiver,” in *Proceedings of the 24th Biennial Symposium on Communications (BSC '08)*, pp. 239–242, June 2008.
- [11] N. K. Mallat and S. O. Tatu, “Six-port receiver in millimeter-wave systems,” in *Proceedings of IEEE International Conference on Systems, Man and Cybernetics*, pp. 2693–2697, Montreal, Canada, October 2007.
- [12] N. K. Mallat, E. Moldovan, and S. O. Tatu, “Comparative demodulation results for six-port and conventional 60 GHz direct conversion receivers,” *Progress in Electromagnetics Research*, vol. 84, pp. 437–449, 2008.
- [13] N. K. Mallat, E. Moldovan, K. Wu, and S. O. Tatu, “High data rate cross-polarized millimeter-wave transmission link,” in *Global Symposium on Millimeter Waves (GSMM '09)*, Katahira Sakura Hall, Tohoku University, April 2009.
- [14] S. O. Tatu, E. Moldovan, K. Wu, and R. G. Bosisio, “A rapid carrier recovery loop for direct conversion receivers,” in *Proceedings of Radio and Wireless Conference (RAWCON '03)*, pp. 159–162, August 2003.
- [15] B. Razavi, “Gadgets gab at 60 GHz,” *IEEE Spectrum*, vol. 45, no. 2, pp. 46–49, 2008.